The evolution of $\sigma^{\gamma P}$ with coherence length

Allen Caldwell

Max Planck Institute for Physics

The content of **arXiv:1601.04472 + a little more**

1 Introduction
2 Data sets & handling
3 Fitting procedures
4 Results
5 Discussion

Update of A.Caldwell, `Behavior of sigma(gamma p) at Large Coherence Lengths', arXiv:0802.0769v1.

inspired by Gribov; `Space-time description of the hadron interaction at high energies', arXiv:0006158v1.

Introduction

View NC scattering in the proton rest frame

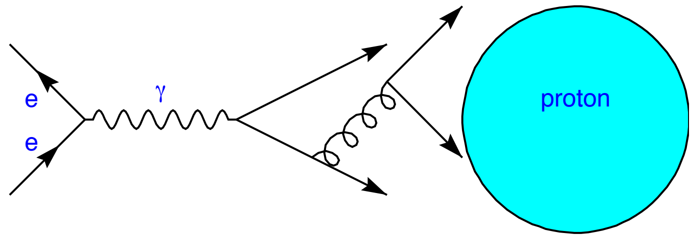

QFT: microscopic world dynamic environment where short-lived states are constantly being created and annihilated. What is the description in the high energy limit ?

DGLAP evolution: evolve from low energy to high… Would like the microscopic model from which we predict behavior at lower energy.

Donnachie-Landshoff observed that the energy dependence of the scattering cross section of high energy hadrons becomes universal. The size of the cross section only depends on the number of valence quarks in the scattering particles and the center-of-mass energy.

Here, study the energy dependence of scattering cross sections for virtual photons on protons. We anticipate that in a high energy limit, the scattering cross sections of virtual photons will also achieve a universal behavior since the interaction will have as source the photon fluctuating into a quark-antiquark pair. Is there a Q^2 independent cross section ? Where does it set in ?

Bjorken Frame: Proton Structure

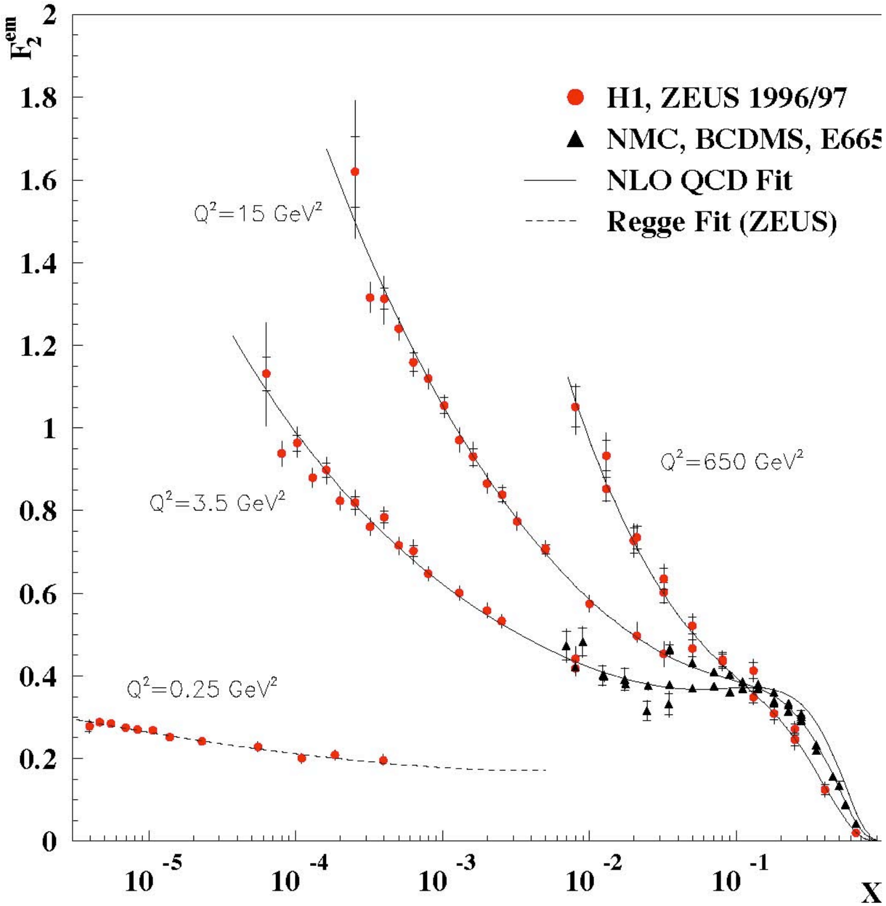

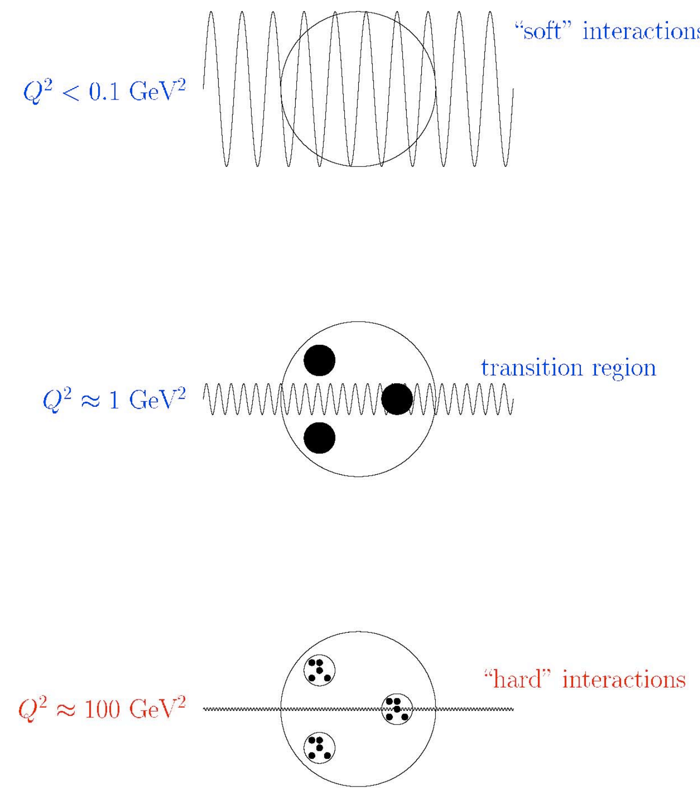

Strong increase in the proton structure function F_2 with decreasing x for fixed, large, Q^2 is interpreted as an increasing density of partons resolved in the proton, providing more scattering targets for the electron.

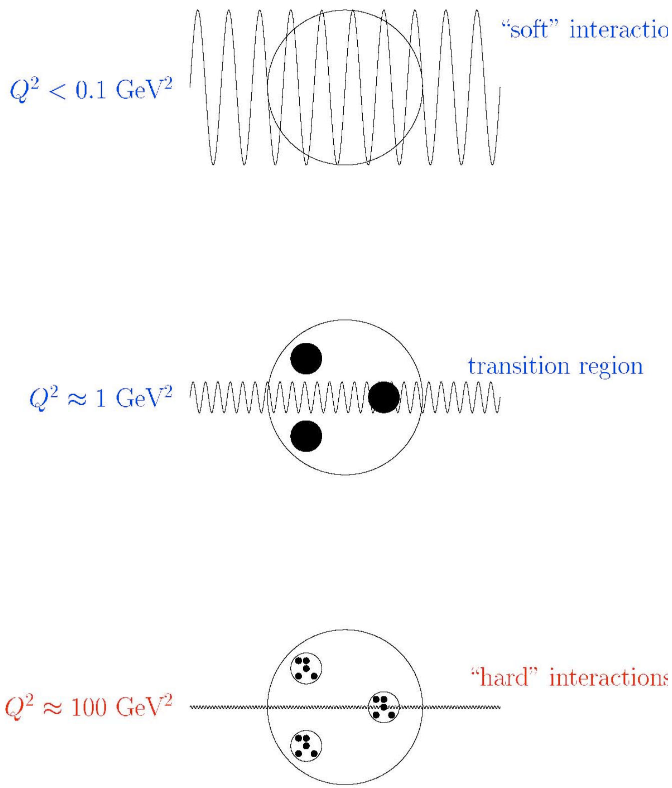

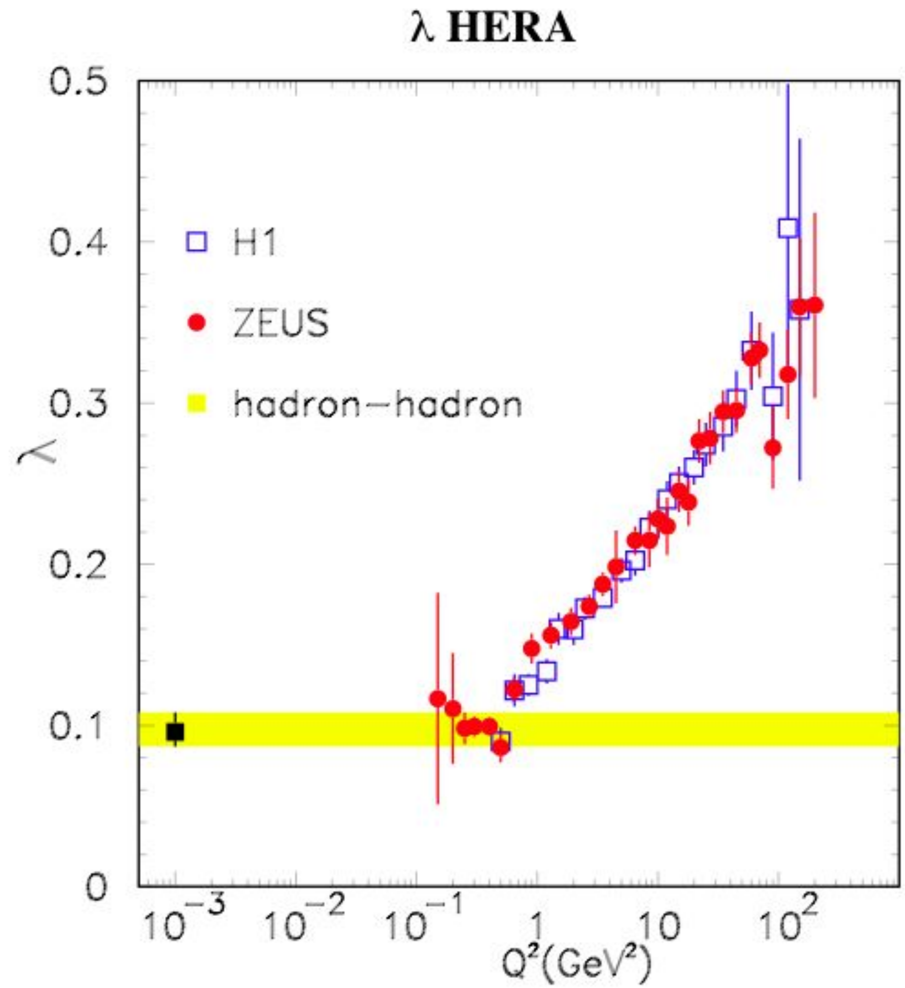

'lambda' plot – Aharon Levy

$$F_2 \propto x^{-\lambda(Q^2)}$$

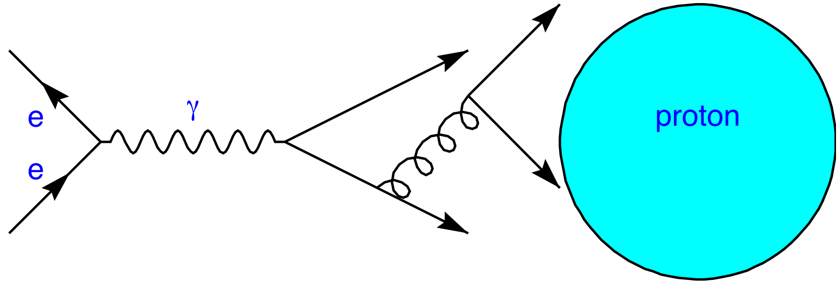

Coherence length of photon fluctuations

$$l \equiv \frac{\hbar c}{\Delta E}$$

where ΔE, the change in energy of the photon as it fluctuates into a system of quarks and gluons, is given by

J. Bartels and H. Kowalski, Eur. Phys. J. C19, 693 (2001).

$$\Delta E \quad \approx \quad \frac{m^2 + Q^2}{2\nu} \tag{1}$$

where ν is the photon energy and m is the mass of the partonic state. For $Q^2 \gg m^2$, we have

$$\Delta E \approx \frac{Q^2}{2\nu} \tag{2}$$

and

$$l \approx \frac{2\nu\hbar c}{Q^2} \approx \frac{\hbar c}{x M_P} \quad . \tag{3}$$

Definition of mass of state into which photon fluctuates defined differently by different authors (including me – previously 2x in denominator)

Data Sets & Handling

1) HERA electron-proton neutral-current scattering data from the ZEUS and H1 experiments
   H. Abramowicz et al., [H1 and ZEUS Collaborations], Eur. Phys. J. C75 1 (2015).

2) Complemented by the small-x data from E665 and NMC
   M. Adams et al. [E665 Collaboration], Phys. Rev. D54, 3006 (1996).
   M. Benvenuti et al. [NMC Collaboration], Nucl. Phys. B483, 3 (1997).

Global Analysis: $0.01 < Q^2 < 500 \ \mathrm{GeV}^2, \, x < 0.01 \text{ and } 0.01 < y < 0.8$

$$\sigma_{\mathrm{red}} = \frac{xQ^4}{2\pi\alpha^2 Y_+} \frac{d\sigma^2}{dx dQ^2} \approx \left[F_2 - \frac{y^2}{Y_+} F_L \right]$$

In total, 45 E665 data points, 13 NMC data points, 23 HERA e^- P data points, and (115, 160, 75, 276) HERA e^+ P data points with E_P =(460,575,820,920) GeV satisfied the selection criteria.

Hand convention
L.N. Hand, Phys. Rev. 129, 1834 (1963). $F_2^P(x, Q^2) = \frac{Q^4(1-x)}{4\pi^2\alpha(Q^2 + (2xM_P)^2)} \sigma^{\gamma P}$

Data Sets & Handling

F_3 can be ignored in the (x,Q^2) range selected for the analysis.

F_2 calculated from the reduced cross section assuming $R=F_L/(F_2-F_L)=0.25$; limit $y<0.8$ to control the possible error due to this assumption.

$x<0.01$ to ensure that we are dealing with large coherence lengths compared to the proton size (>10-20 fm).

The total experimental uncertainties used (statistical and systematic added in quadrature on a point-by-point basis). The use of correlated systematics was investigated but found not to give significant differences for this analysis. In any case, we are looking more for qualitative behavior.

Data Sets & Handling

The data from the different experiments are reported in some cases at fixed values of x and varying Q^2, in other cases at fixed Q^2 and varying x, or at fixed Q^2 and varying y.

The data `bin-centered' by moving data to fixed values of Q^2 using a parametrization

$$F_2(Q_c^2, x) = \frac{F_2^{\rm pred}(Q_c^2, x)}{F_2^{\rm pred}(Q^2, x)} \frac{F_2(Q^2, x)}{S_{\rm expt}}$$

Where $S_{\rm expt}$ is a normalization factor for the experiment in question that resulted from the global fit.

The following Q^2_c values have been used: 0.25, 0.4, 0.65, 1.2, 2, 3.5, 6.5, 10, 15, 22, 35, 45, 90, 120 GeV^2.

Fitting

A. Caldwell, D. Kollar, K. Kröninger, Comput. Phys. Commun. 180, 2197 (2009).

Parametrization for global fit – only needed for ‘bin centering’

Limiting value at small Q^2 and fixed x
Color transparency at large Q^2

$$\sigma_0 \frac{M^2}{Q^2 + M^2}$$

Coherence length dependence

$$\left(\frac{l}{l_0}\right)^{\epsilon_{\rm eff}}$$

with

$$\begin{aligned}
\epsilon_{\rm eff} &= \epsilon_0 && Q^2 \le Q_0^2 \\
\epsilon_{\rm eff} &= \epsilon_1 + \epsilon' \ln\left(Q^2/Q_1^2\right) && Q^2 \ge Q_1^2 \\
\epsilon_{\rm eff} &= \epsilon_0 + (\epsilon_1 - \epsilon_0)\frac{\ln(Q^2/Q_0^2)}{\ln(Q_1^2/Q_0^2)} && Q_0^2 < Q^2 < Q_1^2
\end{aligned}$$

8 parameter form:

$$\sigma^{\gamma p} = \sigma_0 \frac{M^2}{Q^2 + M^2} \left(\frac{l}{l_0}\right)^{\epsilon_{\rm eff}(\epsilon_0, \epsilon_1, \epsilon', Q_0^2, Q_1^2)}$$

+ 1 parameter for normalization of each data set

Parameter	prior function	global mode	68 % interval
σ_0 (mBarns)	$\sigma_0 \sim \mathcal{G}(\circ\|0.07, 0.02)\;\; 0.01 < \sigma_0 < 0.2$	0.062	0.059 – 0.067
M^2 (GeV^2)	$M^2 \sim \mathcal{G}(\circ\|0.75, 0.5)\;\; 0.1 < M_0^2 < 2.0$	0.63	0.59 – 0.67
l_0 (fm)	$l_0 \sim \mathcal{G}(\circ\|1.0, 0.5)\;\; 0.1 < l_0 < 2.0$	1.6	1.54 – 1.77
ϵ_0	$\epsilon_0 \sim \mathcal{G}(\circ\|0.09, 0.01)\;\; 0.05 < \epsilon_0 < 0.2$	0.106	0.102 – 0.110
ϵ_1	$\epsilon_1 \sim \mathcal{G}(\circ\|0.2, 0.2)\;\; 0.1 < \epsilon_1 < 0.3$	0.156	0.152 – 0.160
ϵ'	$\epsilon' \sim \mathcal{G}(\circ\|0.05, 0.02)\;\; 0.0 < \epsilon' < 0.1$	0.052	0.051 – 0.054
Q_0^2 (GeV^2)	$Q_0^2 \sim \mathcal{G}(\circ\|1.0, 1.0)\;\; 0.01 < Q_0^2 < 2.0$	0.37	0.33 – 0.41
Q_1^2 (GeV^2)	$Q_1^2 \sim \mathcal{G}(\circ\|3.0, 3.0)\;\; 2.0 < Q_1^2 < 10.0$	3.13	2.96 – 3.36
$S_{\rm E665}$	$S \sim \mathcal{G}(\circ\|1.0, 0.018)\;\; 0.9 < S_{\rm E665} < 1.1$	0.97	0.958 – 0.982
$S_{\rm NMC}$	$S \sim \mathcal{G}(\circ\|1.0, 0.025)\;\; 0.9 < S_{\rm NMC} < 1.1$	0.94	0.093 – 0.096
$S_{\rm e^-p}$	$S \sim \mathcal{G}(\circ\|1.0, 0.015)\;\; 0.9 < S_{\rm e^-p} < 1.1$	0.997	0.988 – 1.006
$S_{\rm e^+p460}$	$S \sim \mathcal{G}(\circ\|1.0, 0.015)\;\; 0.9 < S_{\rm e^+p460} < 1.1$	1.020	1.014 – 1.030
$S_{\rm e^+p575}$	$S \sim \mathcal{G}(\circ\|1.0, 0.015)\;\; 0.9 < S_{\rm e^+p575} < 1.1$	1.014	1.008 – 1.024
$S_{\rm e^+p820}$	$S \sim \mathcal{G}(\circ\|1.0, 0.015)\;\; 0.9 < S_{\rm e^+p820} < 1.1$	1.009	1.002 – 1.020
$S_{\rm e^+p920}$	$S \sim \mathcal{G}(\circ\|1.0, 0.015)\;\; 0.9 < S_{\rm e^+p920} < 1.1$	0.998	0.992 – 1.008

Photon-Proton Cross Section

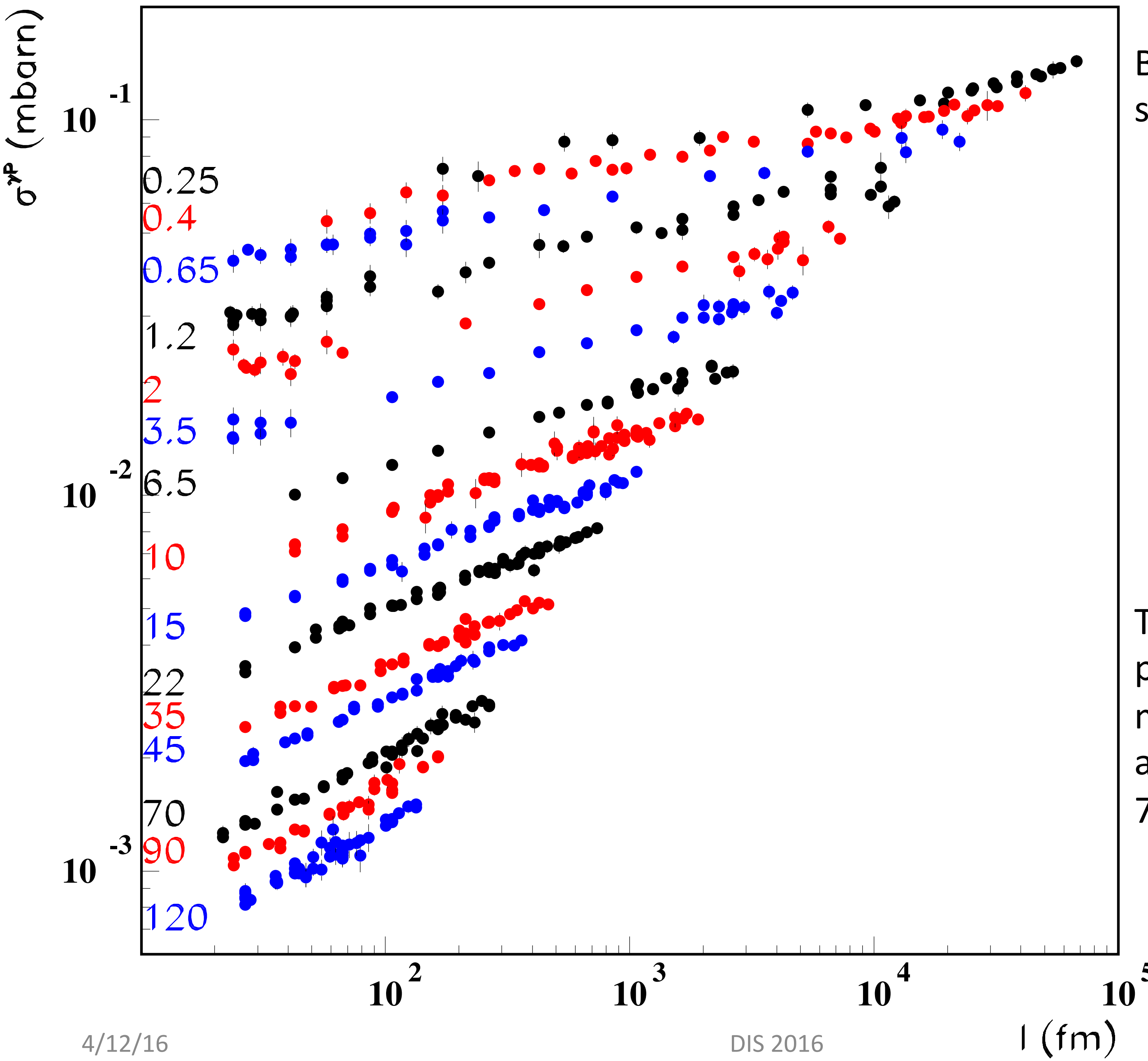

Bin centered cross sections

The posterior probability at the global mode corresponded to a χ^2 value of 761 for 707 fitted data points.

The bin-centered data were then fit to the simple form in the individual Q^2 bins

$$\sigma(l, Q^2) = \sigma_1(Q^2) \left(\frac{l}{1 \text{ fm}} \right)^{\lambda_{\text{eff}}(Q^2)}$$

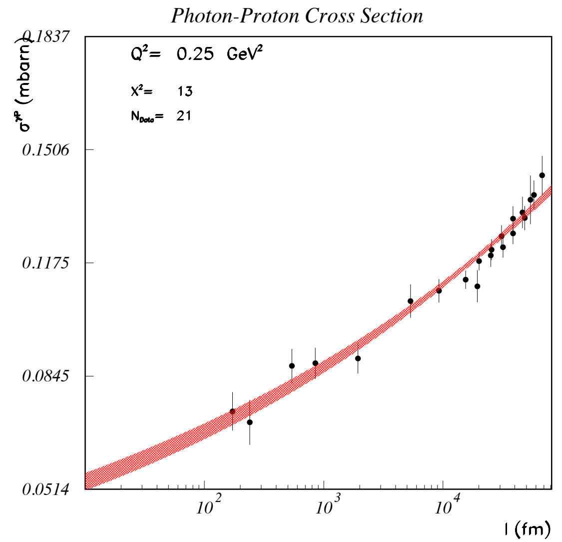

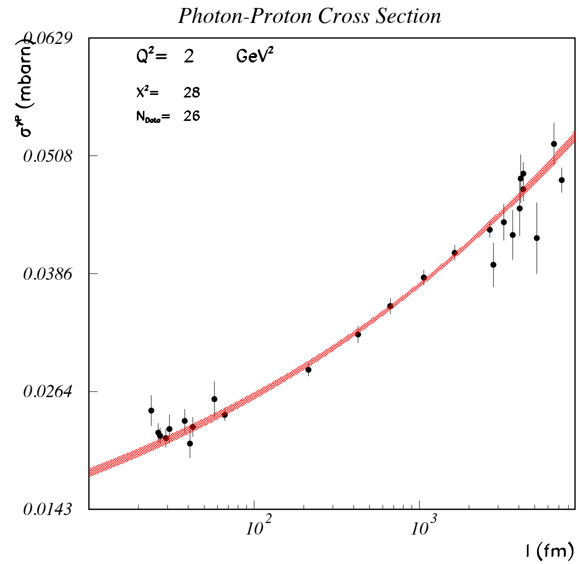

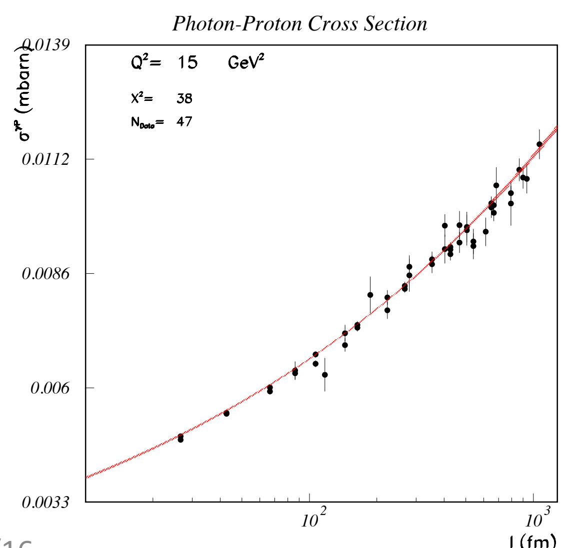

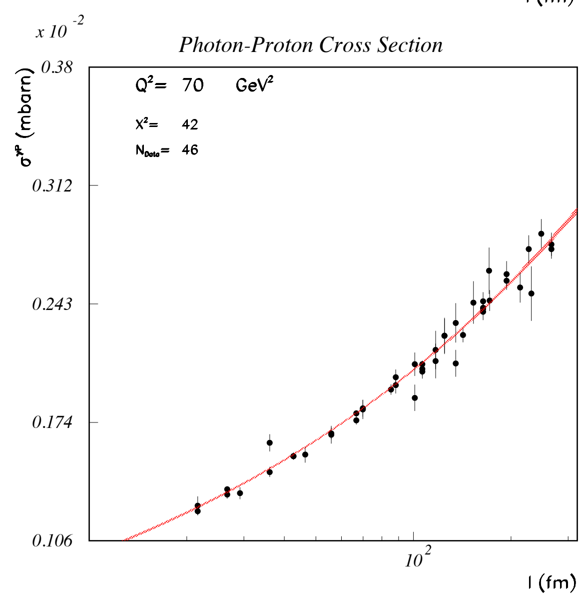

Results

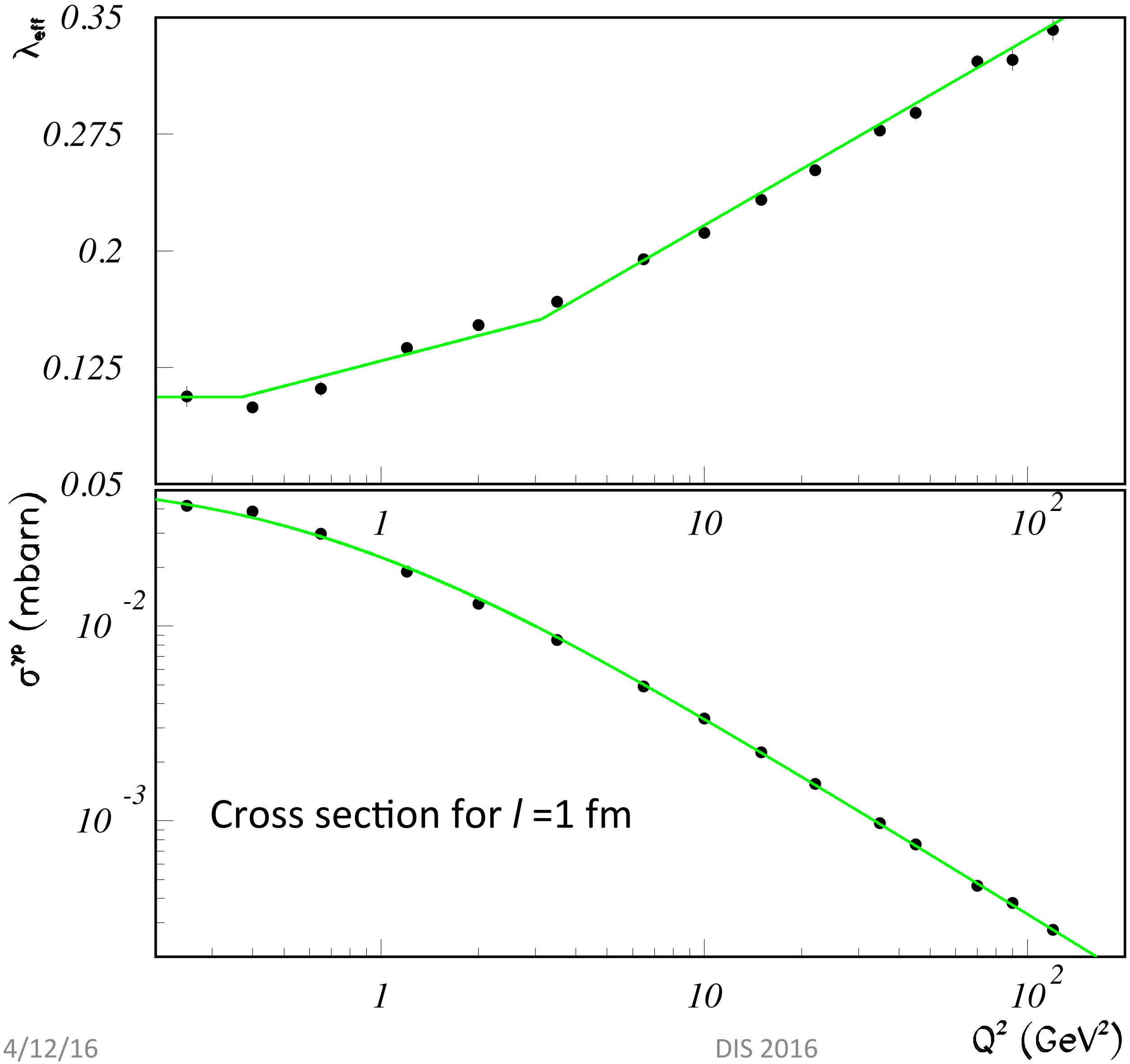

Green curve is from the global fit. Data points are from fits to individual Q^2 bins.

The uncertainties on the fit parameters are typically smaller than then size of the symbols

For $Q^2 > 3\ \mathrm{GeV}^2$, the slope increases in simple way.

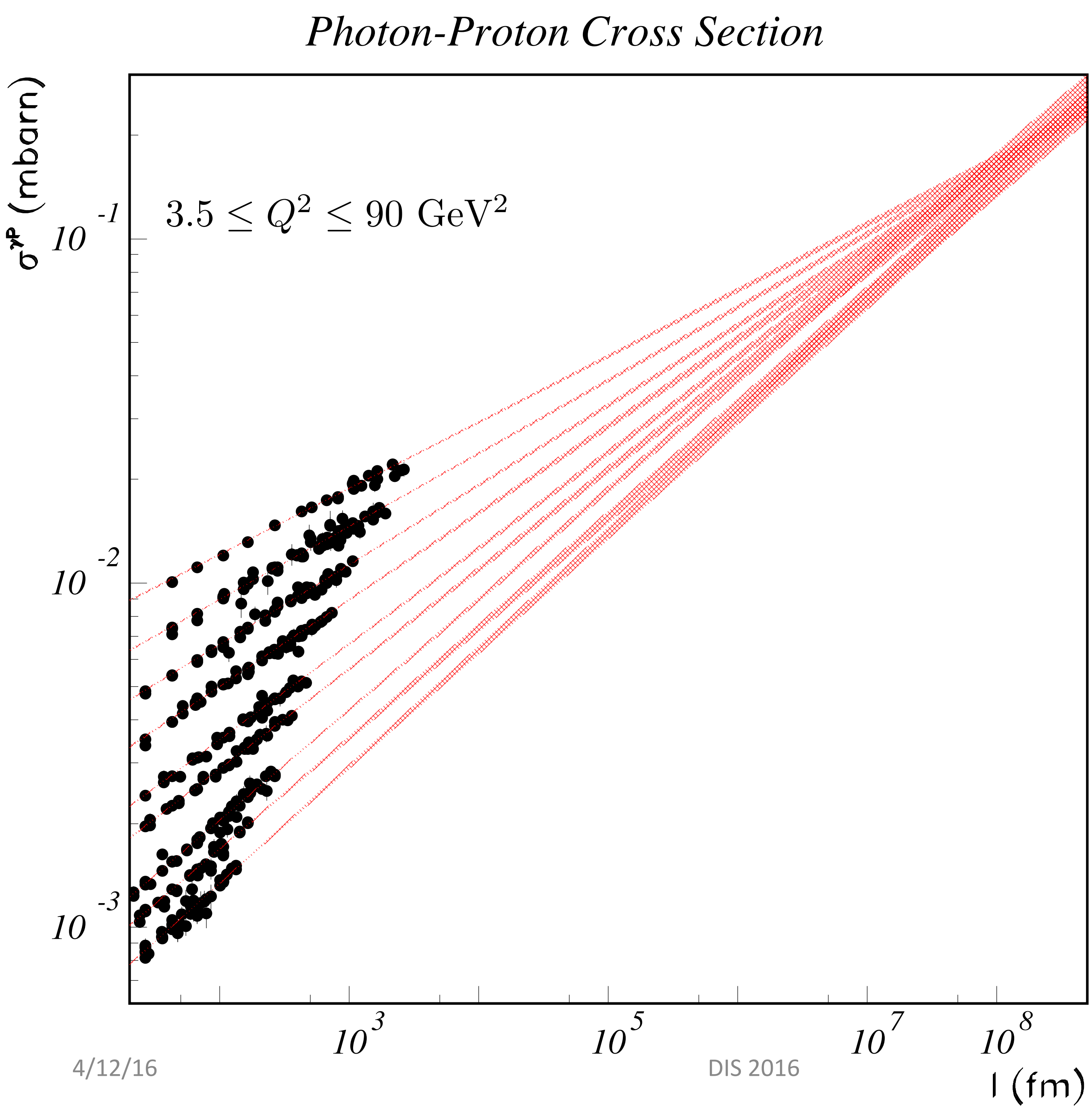

Extrapolated cross sections assuming simple functional form. Large Q^2 cross sections become larger than small Q^2 cross sections.

Alternate fit – Double Asymptotic Scaling (Ball&Forte) inspired form (G. Salam, private communication)

$$\sigma = A \exp^{B \cdot \sqrt{\log(1/x) \log(Q^2/L^2)}}$$

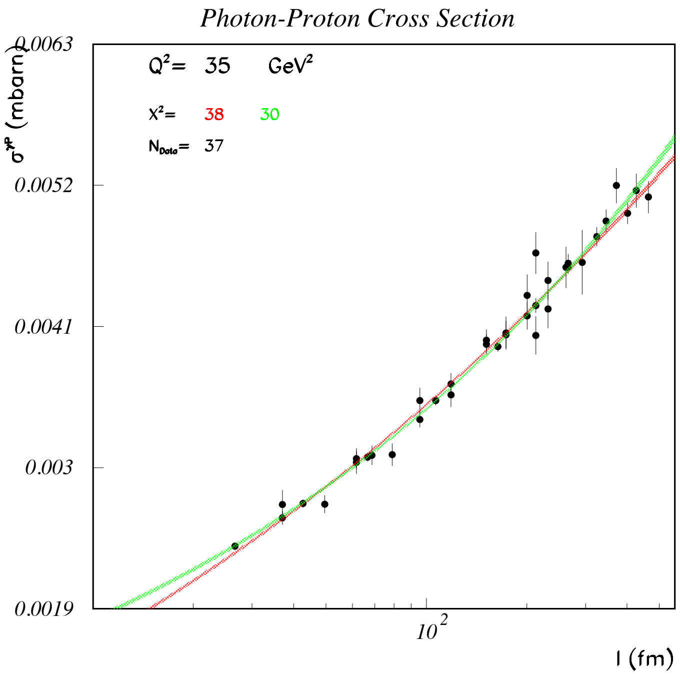

In general – the previous fits give better goodness-of-fit. No crossing with DAS form.

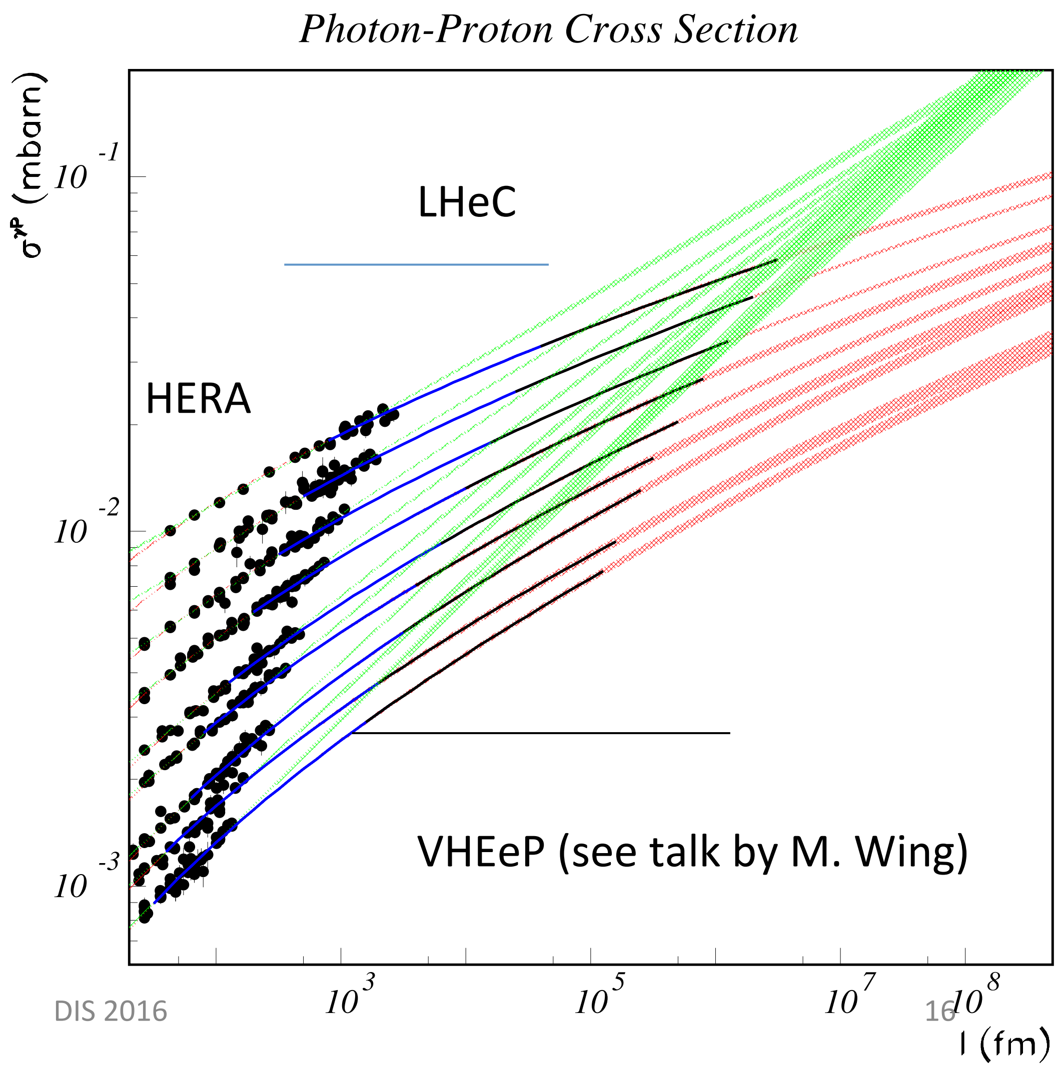

Discussion

Fixed *l*: $\sigma^{\gamma P} \propto \frac{1}{Q^2 + M^2}$ λ_{eff} increases with Q^2

Initially small configurations (large Q^2) will grow to have larger cross section than initially large configurations (small Q^2) if behavior continues unchanged.

Intuition: If the photon states become comparable in size, they should evolve in the same way so that the cross sections evolve uniformly with coherence length, independently of their initial size, and with the same energy dependence as typical for hadronic cross sections.

This hadron-like energy dependence is observed for the smallest Q^2 values investigated (the energy dependence is the same as for hadron-hadron scattering).

We therefore expect that the slope of the cross section with coherence length should flatten as a function of coherence length; this could be an indication for saturation of the parton densities.

Discussion

İt is also possible that the power law behavior of the cross section changes with coherence length without saturation (e.g., DAS or Kowalski, Lipatov, Ross arXiv:1508.05744), but this would again imply an interesting change in gluon dynamics. The new effects should set in below $l = 10^8\ \mathrm{fm}$ to avoid the cross sections crossing.

First signs of the change in slope would presumably set in considerably earlier. The approach to saturation and a fundamentally new state of matter is therefore perhaps within reach of next generation lepton-hadron colliders such as LHeC or VHEeP, an exciting prospect.

HERA data has shown an exciting prelude to fundamental physics – let's go for it.